J Physiol 588.5 (2010) pp 861–872

Zebrafish (*Danio rerio*) gill neuroepithelial cells are sensitive chemoreceptors for environmental CO_2

Z. Qin, J. E. Lewis and S. F. Perry

Department of Biology, University of Ottawa, 30 Marie Curie Street, Ottawa, Canada ON K1N 6N5

Adult zebrafish exhibit hyperventilatory responses to absolute environmental CO_2 levels as low as 0.13% (P_{CO_2} = 1.0 mmHg), more than an order of magnitude lower than the typical arterial P_{CO_2} levels (~40 mmHg) monitored by the mammalian carotid body. The sensory basis underlying the ability of fish to detect and respond to low ambient CO_2 levels is not clear. Here, we show that the neuroepithelial cells (NECs) of the zebrafish gill, known to sense O_2 levels, also respond to low levels of CO_2. An electrophysiological characterization of this response using both current and voltage clamp protocols revealed that for increasing CO_2 levels, a background K^+ channel was inhibited, resulting in a partial pressure-dependent depolarization of the NEC. To elucidate the signalling pathway underlying K^+ channel inhibition, we used immunocytochemistry to show that these NECs express carbonic anhydrase (CA), an enzyme involved in CO_2 sensing in the mammalian carotid body. Further, the NEC response to CO_2 (magnitude of membrane depolarization and time required to achieve maximal response), under conditions of constant pH, was reduced by ~50% by the CA-inhibitor acetazolamide. This suggests that the CO_2 detection mechanism involves an intracellular sensor that is responsive to the rate of acidification associated with the hydration of CO_2 and which does not require a change of extracellular pH. Because some cells that were responsive to increasing P_{CO_2} also responded to hypoxia with membrane depolarization, the present results demonstrate that a subset of the NECs in the zebrafish gill are bimodal sensors of CO_2 and O_2.

(Resubmitted 23 November 2009; accepted after revision 4 January 2010; first published online 5 January 2010)
Corresponding author S. F. Perry: Department of Biology, University of Ottawa, 30 Marie Curie, Ottawa, ON, Canada K1N 6N5. Email: sfperry@uottawa.ca

Abbreviations CA, carbonic anhydrase; NEC, neuroepithelial cell.

Introduction

In a wide range of animal species, the ability to sense environmental CO_2 plays an integral role in homeostasis. In mammals, CO_2 sensing occurs centrally (brainstem neurons) and in the periphery (carotid body) (O'Regan & Majcherczyk, 1982; Gonzalez *et al.* 1992; Lahiri & Forster, 2003). The Type 1 glomus cells of the carotid body appear to be the primary sensors of CO_2 in the peripheral circulation (Lahiri & Forster, 2003). Although it has been long thought that peripheral CO_2 sensing in vertebrates first evolved in air-breathers, evidence is mounting that fish also sense CO_2 in their environment (Burleson & Smatresk, 2000; Reid *et al.* 2000; Sundin *et al.* 2000; McKendry *et al.* 2001; Perry & Reid, 2002; see reviews by Milsom *et al.* 1999; Gilmour, 2001; Perry & Gilmour, 2002; Gilmour & Perry, 2007). The gill, which is typically the predominant site of respiratory gas transfer in fish as well as the established site of O_2 chemoreception (Smith & Jones, 1978), is now also recognized as the principal site of CO_2 sensing (Perry & Gilmour, 2002; Gilmour & Perry, 2007). The similarity between the gill and carotid body in the sensing of gases is consistent with the evolutionary origin of the carotid body, namely the chemoreceptor cells of the first branchial arch (Milsom, 2002; Milsom & Burleson, 2007).

Although fish, like other vertebrates, possess central and peripheral (gill) CO_2 chemoreceptors, the central receptors appear to be confined to air-breathing species (Milsom, 2002). Based on the few whole animal studies that have been performed, it would appear that gill chemoreceptors are specifically sensitive to CO_2 rather than H^+ (Perry *et al.* 1999; Reid *et al.* 2000; Sundin *et al.* 2000; Perry & McKendry, 2001; McKendry & Perry, 2001; Gilmour *et al.* 2005). Unlike air breathers, which maintain high P_{CO_2} levels (e.g. ~40 mmHg in mammals) in arterial blood relative to ambient air, fish achieve arterial P_{CO_2} (P_{aCO_2}) levels which are near ambient and approximately an order of magnitude lower (~2–3 mmHg). Thus, CO_2 detection systems in fish presumably have evolved to sense deviations

DOI: 10.1113/jphysiol.2009.184739

in P_{CO_2} from a very low set point. Moreover, because of the log-linear relationship between pH and P_{CO_2}, equivalent changes in P_{aCO_2} will produce larger changes in arterial pH in fish (resting $P_{aCO_2} = 2-3$ mmHg) than in mammals (resting $P_{aCO_2} = 40$ mmHg). The potentially disruptive effects of small changes in P_{aCO_2} in fish on acid–base balance reinforces the need for piscine CO_2 sensors to detect small changes in P_{CO_2} deviating from a low set point. Indeed, a recent study demonstrated hyperventilatory responses in zebrafish (*Danio rerio*) to environmental CO_2 levels of 0.13% ($P_{CO_2} = 1.0$ mmHg; Vulesevic *et al.* 2006), which would have increased P_{aCO_2} by approximately 1 mmHg. Thus, studying fish provides an opportunity to compare mechanisms of CO_2 sensing in animal systems that have evolved under very different constraints; the low P_{CO_2} system in fish *versus* the high P_{CO_2} system in mammals.

The neuroepithelial cell (NEC), first described in the fish gill by Dunel-Erb *et al.* (1982), was recently identified as an O_2 chemoreceptor in zebrafish (Jonz *et al.* 2004) and channel catfish (*Ictalurus punctatus*) (Burleson *et al.* 2006) using patch clamp techniques. The NECs are enriched with neurotransmitters (Zaccone *et al.* 1989, 1992; Goniakowska-Witalinska *et al.* 1995; Zaccone *et al.* 1997, 2006), are extensively innervated (Bailly *et al.* 1992; Jonz & Nurse, 2003; Saltys *et al.* 2006) and bear striking resemblance to the glomus cells of the mammalian carotid body (Gonzalez *et al.* 1994) that are recognized to function as both O_2 and CO_2 sensors in mammals (Lahiri & Forster, 2003). These similarities, as well as the proposed evolutionary relationship between the carotid body and fish gill chemorecetors, suggest that NECs might also be sensitive to both O_2 and CO_2. Although there are convincing data demonstrating that NECs act as O_2 sensors (Jonz *et al.* 2004; Burleson *et al.* 2006), evidence implicating NECs as CO_2 chemoreceptors is lacking.

Here, we use patch clamp electrophysiology to show that a subset of NECs in the zebrafish gill, previously shown to be responsive to O_2, can also act as sensitive CO_2 sensors. The threshold P_{CO_2} level is an order of magnitude lower than for both mammalian carotid body glomus cells and brainstem neurons (Guyenet, 2008). Further, we show that the transduction mechanism is mediated by a carbonic anhydrase (CA)-dependent inhibition of a background K^+ conductance, and can occur independently of any change in extracellular pH.

Methods

Animals

Adult zebrafish (*Danio rerio*) were obtained from a commercial supplier (MIRDO, Montreal, Canada) and transported to the University of Ottawa Aquatic Care Facility where they were maintained in acrylic tanks (4 l) supplied with aerated, dechloraminated City of Ottawa tap water at 28°C. Fish were maintained on a constant 10 : 14 light–dark photoperiod. All procedures for animal use were approved by the University of Ottawa Animal Care and Veterinary Service and carried out according to institutional guidelines and in accordance with those of the Canadian Council on Animal Care (CCAC). The procedures comply with guidelines for reporting of ethical matters in *The Journal of Physiology* as outlined by Drummond (2009).

Cell isolation and immunocytochemistry

Zebrafish were decapitated after a sharp blow to the head. All procedures for isolation of NECs were carried out under sterile conditions in a laminar flow hood (Jonz *et al.* 2004). Gill baskets were removed and rinsed in a wash solution (2% penicillin–streptomycin in phosphate-buffered saline (PBS)) for 10 min. All eight gill arches were then separated and distal filaments rich in NECs (Jonz *et al.* 2004) were selectively removed. Tissue was placed in 0.01% hyaluronidase for 10 min then 0.25% trypsin/EDTA (Invitrogen Corp.) for 1 h at room temperature, minced with fine forceps and triturated in a 15 ml centrifuge tube with a Pasteur pipette. The trypsin reaction was stopped with the addition of 10% fetal calf serum (FCS). Lower concentrations of trypsin or mechanical separation alone did not work well for dissociation. The cell suspension was centrifuged (140 *g*) for 5 min and the pellet triturated in PBS. Gill cells were centrifuged once more with PBS and suspended in Leibovitz's (L-15, with L-glutamine but without phenol red) culture medium supplemented with 1% penicillin–streptomycin and 5% FCS.

For the immunocytochemical studies of NECs in culture, cells were plated on sterile CellBIND culture dishes (Corning Inc., New York; Ryan, 2005) for 24–48 h after dissociation, followed by fixation with 4% paraformaldehyde (PFA) in PBS for 15 min at room temperature and immunolabelled using mouse monoclonal anti-5-hydroxytryptamine (5HT) pre-diluted antibodies (1 : 1, Biomeda Corp., Foster City, CA, USA) in conjunction with polyclonal human CA II antibodies (1:100, Rockland Immunochemicals, Gilbertsville, PA, USA). Monoclonal 5HT antibodies were visualized with goat anti-mouse secondary antibodies conjugated with Alexa 546 (1 : 400, Molecular Probes, Eugene, OR, USA). Polyclonal CA antibodies were localized with goat anti-rabbit secondary antibodies conjugated with Alexa 488 (1 : 400, Molecular Probes). All antibodies were diluted with PBS containing 0.5% Triton X-100 (PBST). Fixed cells were incubated in primary antibody for 2 h, followed by immersion in secondary antibody in darkness for 1 h at room temperature. Labelled cells were washed (3 × 5 min) and mounted with media containing

4′,6′-diamidino-2-phenylindole (DAPI) to stain nuclei (Vectashield, Vector Laboratories, Inc., Burlingame, CA, USA). Cells were observed and photographed using a Zeiss Axiophot fluorescence microscope and a Hamamatsu C5985 chilled CCD camera (East Syracuse, NY, USA). Images were captured using Metamorph imaging software (v. 4.01). Observations were performed using at least 10 cell culture dishes unless stated otherwise and the results obtained were consistently reproduced. To verify the specificity of the 5HT and CA antibodies, control experiments were conducted in which NECs were incubated with PBS lacking primary antibodies or immersed in primary antibodies preabsorbed for 30 min with excess antigen (40 μg μl^{-1} 5HT for 5HT antibody or 50 μg μl^{-1} bovine CA for CA antibody). The specificity of the human CA II antibody against the zebrafish orthologue (zCAc; see Gilmour & Perry, 2009) was established in preliminary experiments in which western blotting revealed that the human antibody detected single zebrafish and rat proteins of similar size (29 kDa). Furthermore, a CA antibody (Georgalis *et al.* 2006) developed against rainbow trout cytosolic CA (tCAc; Esbaugh *et al.* 2005) was equally effective at detecting a 29 kDa zebrafish protein. We opted to use the human rather than the trout antibody in the present study because it yielded higher quality (less background) immunocytochemistry images.

Electrophysiology

Whole-cell recordings (Hamill *et al.* 1981) were performed *in vitro* using zebrafish gill cell culture preparations, essentially as described previously (Jonz *et al.* 2004). Specialized 35 mm culture dishes (see above, Corning Inc.) were plated with dissociated NECs. After 24 and 48 h, NECs that adhered to the culture substrate were identified using 2 mg ml^{-1} Neutral Red (NR; Sigma), a vital marker used to identify NECs (Jonz *et al.* 2004). Based on observation and measurement of NECs *in vitro*, larger NR-positive cells (≥ 7 μm in diameter) were selected for electrophysiological recording. Later on, dishes were mounted on a fixed stage of a Zeiss inverted microscope and a perfusion insert (Warner Instruments, LLC, Hamden, CT, USA) with inlet and outlet was placed in it. Patch electrodes were fabricated from borosilicate glass with filament (1.5 mm o.d.; 0.86 mm i.d.; 10 cm length; Sutter Instrument Co., Novato, CA, USA). Glass electrodes were pulled on a horizontal pipette puller (P-2000, Sutter Instrument Co.) and filled with pipette (intracellular recording) solution containing (mM): KCl 135, NaCl 5, $CaCl_2$ 0.1, EGTA 11, Hepes 10 and Mg-ATP 2; pH adjusted to 7.2 with KOH; resulting tip resistances were typically 5–7 MΩ. Bath (extracellular) solution contained (mM): NaCl 135, KCl 5, $CaCl_2$ 2, $MgCl_2$ 2, glucose 10 and Hepes 10; pH adjusted to 7.4 with NaOH. Seal resistance was typically more than 5 GΩ and holding current was less than 5 pA at −60 mV.

Voltage-clamp protocols were performed using a MultiClamp 700B amplifier (Molecular Devices, Sunnyvale, CA, USA) interfaced with an IBM PC, data acquisition system (DigiData 1322A, Molecular Devices) and Clampex 9.2 software (Molecular Devices). Under voltage-clamp, cells were typically held at −60 mV and currents were evoked either by changing the membrane potential from −100 mV (or −90 mV) to +60 mV over a period of 1 s (ramp protocol) or by delivering a step command (+30 mV for 50 ms) every 10 s from a holding potential of −60 mV. In the latter cases, steady-state current was measured as the average current evoked between 40 and 49 ms of each 50 ms voltage step interval. Current-clamp recordings were performed using the same apparatus. All recordings were filtered at 5 kHz and digitized at 10 kHz. In some cases, acquired signals were additionally filtered using an 8-pole Bessel filter (cut off at 200 Hz) to remove high frequency noise. All data were analysed using Clampfit 9.0 software (Molecular Devices). In Fig. 4*B*, the Goldman–Hodgkin–Katz current equation (eqn (14.5), p. 445, Hille, 2001) was used to describe the CO_2-sensitive current as a function of membrane voltage, with $P_K = 2.5 \times 10^{-6}$, $[K^+]_i = 135$ mM, $[K^+]_o = 5$ mM.

The recording chamber was continuously perfused (4 ml min^{-1}) with bath solution at room temperature (22–24°C) using a constant pressure head and a four-channel remote valve control system (ALA Scientific Instruments Inc., Farmingdale, NY, USA). Hypoxia was produced by bubbling N_2 through standard extracellular recording solution in the perfusion reservoir (60 ml syringe) for at least 15 min until the desired P_{O_2} (15–17 mmHg) was reached. This degree of hypoxia was slightly greater than that used by Jonz *et al.* (2004; 25 mmHg) but consistent with estimated arterial P_{O_2} levels in zebrafish experiencing a maximal hyperventilatory response during acute hypoxia (Vulesevic *et al.* 2006). Different levels of hypercapnia were produced by bubbling commercially produced CO_2 mixtures (0.25%, 0.5% or 1% CO_2 balanced with air; BOC Canada Ltd) through the extracellular recording solution in the perfusion reservoir (60 ml syringe) until water P_{CO_2} reached equilibrium. Water P_{CO_2} was measured using a CO_2 electrode (Cameron Instrument Co., Guelph, Ontario, Canada; model E201) connected to a Cameron BGM 200 blood gas meter. Measurements of O_2 were made using a fibre optic oxygen electrode (Ocean Optics Foxy AL300, Dunedin, FL, USA) and associated hardware and software (Ocean Optics SD 2000). Gas impermeable tubing (Tygon, Saint-Gobain Performance Plastics Corp., Akron, OH, USA) was used to transfer the perfusate to the recording chamber. Control experiments were performed in which the perfusate was bubbled with air.

Two conventional blockers of K^+ channels were used to characterize the CO_2 sensitive current. 4-AP (2.5 mM) was used to block voltage-gated K^+ channels while quinidine (0.5 mM) was used to block background K^+ channels. To assess the importance of CA activity in CO_2 sensing, cells were exposed to the membrane-permeant CA blocker, acetazolamide (50 μM). All drugs were purchased from Sigma and dissolved in the extracellular bath solution (pH adjusted to 7.4).

Statistical analysis

Data acquired under conditions of current or voltage clamp are presented as means ± S.E.M. Differences between treatments were analysed using Student's *t* test for paired data or one-way repeated measures ANOVA followed by Bonferroni's *post hoc* test for multiple comparisons. Significance was accepted if $P < 0.05$. Statistical analyses of data were performed using commercial software (SigmaStat v. 3.1; SPSS).

Results

Effects of hypercapnia or hypoxia on NEC membrane potential under current-clamp recording

NECs exhibited membrane depolarization when treated with hypoxic (Hox; $P_{O_2} = 17$ mmHg) or hypercapnic (Hpc; 1% CO_2; $P_{CO_2} = 7.5$ mmHg) solutions (Fig. 1). In 18 cells (of 30 cells tested), there was a significant change in membrane potential (V_m) from -54.8 ± 1.8 to -28.8 ± 4.6 mV (paired *t* test, $P < 0.001$) after bath perfusion with hypercapnic solution (Fig. 1*D*). The 12 unresponsive cells were not tested for their O_2 sensitivity. In another set of experiments, six cells (of 18 cells tested) responded to both elevated CO_2 and reduced O_2 (Fig. 1*B* and *C*). NECs exposed sequentially to hypercapnia, allowed to recover and then exposed to hypoxia displayed similar increases in V_m (Fig. 1*E*). The change in the membrane potential outlasted the hypercapnic/hypoxic treatment to a varying degree.

Dose-dependent effects of hypercapnia on NECs under current-clamp recording

Figure 2*A*, *B* and *C* show typical V_m traces of the reversible depolarization recorded from a single NEC when exposed sequentially to bath perfusates equilibrated with 0.25%, 0.5% or 1% CO_2. Figure 2*D* shows the mean values of V_m at the three different levels of P_{CO_2}. Clearly, hypercapnic stimuli evoked NEC membrane depolarization in a dose (partial pressure)-dependent manner.

Temporal effects of hypercapnia on NECs under voltage-clamp recording

While there was a clear dose dependence of the NEC response to hypercapnia, the response onset times were

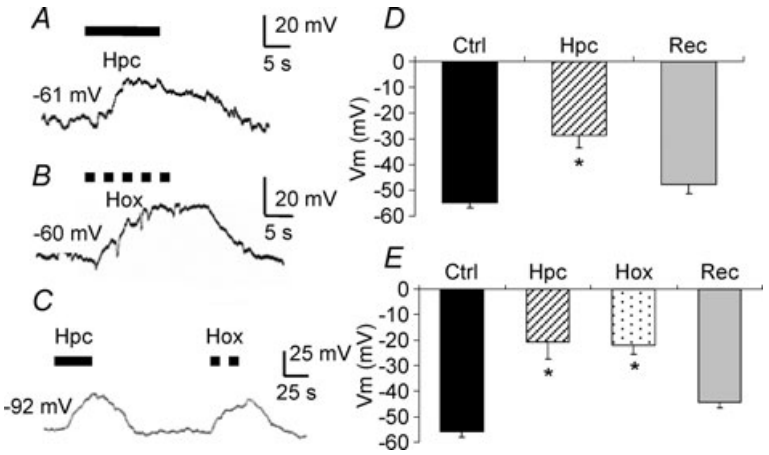

Figure 1. Effects of hypercapnia or hypoxia on membrane potential in isolated cultured gill neuroepithelial cells (NECs) of zebrafish (*Danio rerio*)
A and *B*, typical current clamp recordings showing membrane depolarization during perfusion with hypercapnic (Hpc, 1% $CO_2 = 7.5$ mmHg, continuous line) or hypoxic solutions (Hox, $P_{O_2} = 17$ mmHg, dashed line), respectively. *C*, current clamp recording showing depolarization during perfusion with hypercapnic (filled arrow bar) or hypoxic solution (dashed bar) measured on the same cell. *D*, mean ± S.E.M. ($n = 18$ cells) membrane potential (V_m) of NECs during perfusion with control (Ctrl) or hypercapnic (Hpc) solutions, and subsequent recovery (Rec). V_m was significantly reduced by 26 mV during hypercapnia (paired *t* test, $^*P < 0.001$). *E*, mean ± S.E.M. ($n = 6$) V_m of NECs for sequential stages of control, hypercapnia, hypoxia (Hox) and recovery during recording from the same cell. V_m was significantly and reversibly reduced in the presence of hypercapnia and hypoxia relative to controls (one-way repeated measures ANOVA, $^*P < 0.001$).

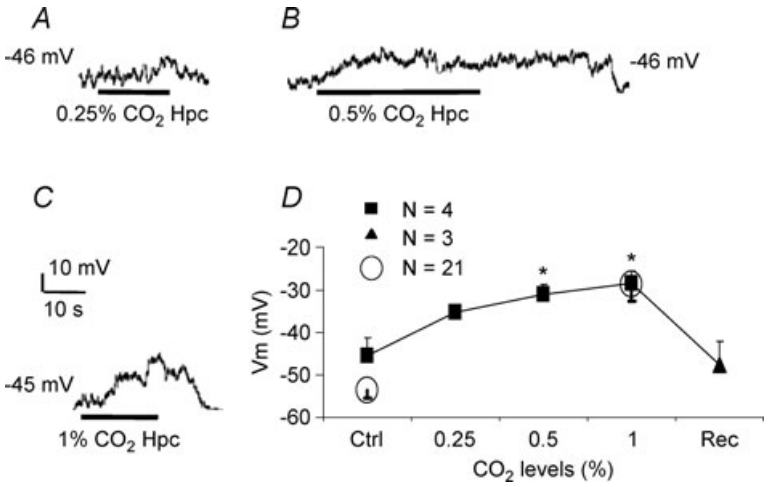

Figure 2. Dose (P_{CO_2})-dependent effects of hypercapnia on membrane potential in isolated cultured neuroepithelial cells (NECs) of zebrafish (*Danio rerio*)
A–C, representative traces of reversible depolarization of the same NEC during perfusion (bar) with hypercapnic solutions, 0.25% (P_{CO_2} = 1.9 mmHg), 0.5% (P_{CO_2} = 3.8 mmHg) or 1% (P_{CO_2} = 7.5 mmHg) CO_2. Scale bar = 10 mV/10 s in *C* (applies to *A* and *B* as well). *D*, mean ± S.E.M. values of membrane potential (V_m) during hypercapnia. Continuous line and filled squares show the dose-dependent trend of V_m during hypercapnia on the same set of NECs ($n = 4$; filled triangle for recovery $n = 3$; one-way repeated measures ANOVA *versus* control, $^*P < 0.05$). Open circles represent data from NECs using control and 1% CO_2 alone ($n = 21$).

variable. To address this issue directly, voltage clamp protocols were used to measure the responses of NECs before, during (10–30 s) and after the perfusion of the hypercapnic solution. Typical whole-cell currents and average values of inhibition in NECs ($n = 6$) are shown in Fig. 3, where currents were evoked using a voltage step protocol from −60 mV to 30 mV every 10 s. The reduction in current over time under these conditions was similar to the dose-dependent change in membrane potential under current clamp (during bath perfusion with different levels of hypercapnia, Fig. 2*D*). This provides further evidence of a dose response and suggests that much of the time dependence in the response onset is due to the delay in reaching the target P_{CO_2}. The data depicted in Figs 2 and 3 may actually underestimate the cellular responses of NECs to CO_2 because the need for rapid experimentation on the fragile cells meant that steady-state responses were not always achieved.

NECs express a CO_2-sensitive outward current

Under voltage clamp, NECs expressed an outwardly rectifying current that was sensitive to changes in P_{CO_2}. Figure 4*A* depicts the average current–voltage (*I–V*)

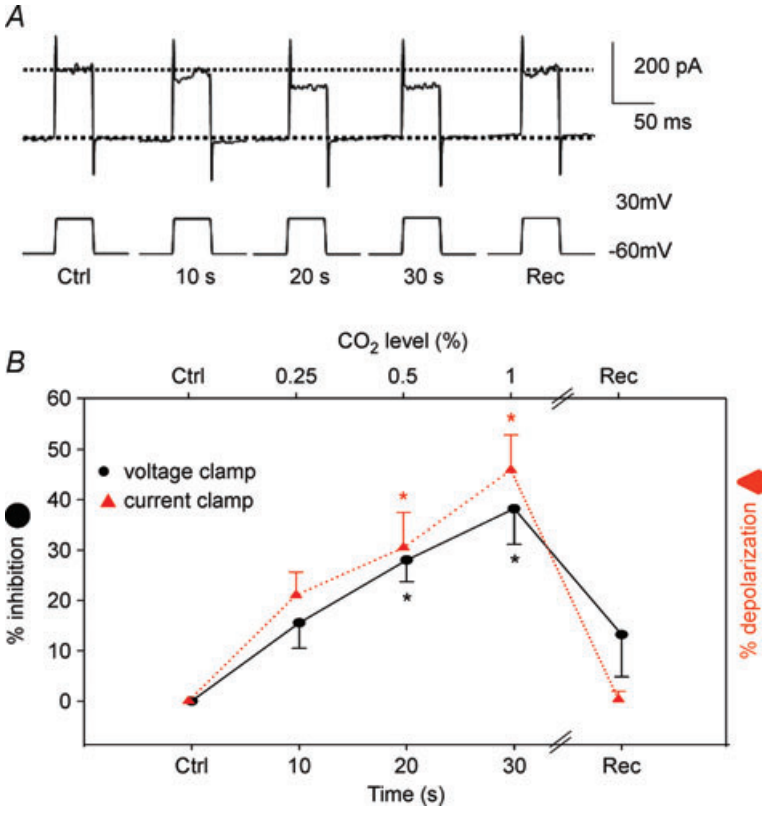

Figure 3. Time-series effects of hypercapnia-induced current in cultured gill neuroepithelial cells (NECs) of zebrafish (*Danio rerio*) under voltage-clamp (V_{clamp}) recording
A, representative whole cell current traces evoked every 10 s using voltage steps from −60 to 30 mV before, at times 10–30 s of hypercapnia and during recovery, respectively. *B*, mean ± S.E.M. ($n = 6$) percentage of steady state current inhibition before, at times 10–30 s of hypercapnia and during recovery (continuous line with filled circles). For comparison, dashed line and triangles show mean ± S.E.M. values of percentage of membrane potential (V_m) depolarization (data taken from Fig. 2*D*) during bath perfusion with different levels of hypercapnia under current clamp (one-way repeated measures ANOVA *versus* control, $^*P < 0.05$).

relationship from 12 NECs (obtained using a ramp protocol, −90 to 60 mV, inset) under control and hypercapnic conditions. The inhibitory effects of hypercapnia on outward currents were apparent over a broad range of membrane potential (from −60 mV to 60 mV), and when measured at 50 mV ranged from 21 to 51% with an average inhibition of 36% ($n = 12$). Figure 4*B* shows the mean CO_2-sensitive difference current (Nox – Hpc) from the same 12 cells. The CO_2-sensitive current reverses near the potassium equilibrium potential, E_K (calculated as −83 mV in the present conditions) and is well-described by the Goldman–Hodgkin–Katz (GHK) current equation, suggesting that it is mediated by background potassium channels (referred to here as I_{KCO_2}).

Pharmacological characterization of the CO_2 sensitive current I_{KCO_2}

The K^+ channel blockers 4-AP and quinidine were used to pharmacologically characterize the CO_2 sensitive current. CO_2 sensitive NECs were first identified by the occurrence of hypercapnic inhibition of the outward current evoked by a ramp protocol under voltage clamp ($n = 5$, Fig. 5*A*). A decrease in whole cell outward current was also observed with 2.5 mM 4-AP alone (indicating the presence of voltage-dependent potassium channels in NECs). However, subsequent hypercapnia caused further inhibition (proportionately similar to that observed with hypercapnia alone; compare Nox with Hpc and 4-AP with 4-AP+Hpc in Fig. 5*A*), suggesting that I_{KCO_2} was not carried by voltage-dependent K^+ channels. This conclusion was further supported by current clamp recordings. Figure 5*B* depicts membrane depolarization of a NEC after application of 2.5 mM 4-AP followed by a further membrane depolarization during exposure to hypercapnia.

Application of 0.5 mM quinidine reduced currents over a range of membrane potentials, but a subsequent hypercapnia had little effect (Quid+Hpc; $n = 6$, Fig. 5*C*). Again, these data are corroborated by current-clamp recordings. Figure 5*D* shows that in a single NEC, the prominent depolarization under bath application of 0.5 mM quinidine prevented further depolarization during hypercapnia. A summary of the I_{KCO_2} sensitivity to quinidine and insensitivity to 4-AP is shown in Fig. 5*E*, and suggests that background K^+ channels in NECs underlie I_{KCO_2}.

Carbonic anhydrase mediates the NEC responses to hypercapnia

Hypercapnia is associated with decreased pH in the extracellular fluids and thus could act through a pH sensor rather than an intracellular CO_2-mediated CA-dependent intracellular process. We first tested for the presence of CA using immunocytochemistry. Representative images of 5HT immunoreactivity (IR) and/or CA-IR NECs in primary cell culture are depicted in Fig. 6*A*. Although all 5HT-IR cells (NEC) exhibited CA-IR, some cells appeared to exclusively express CA (data not shown). If NECs were

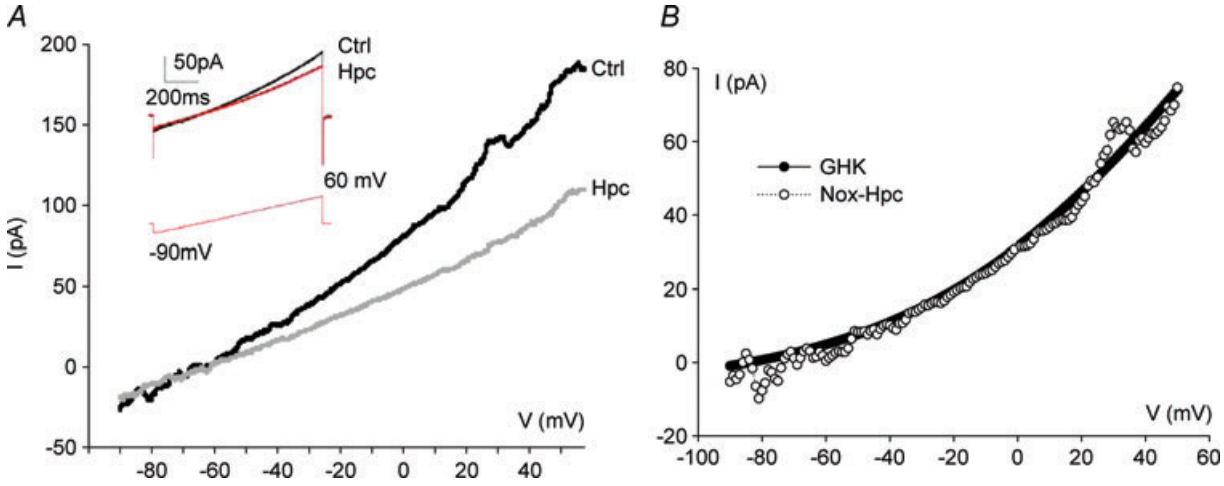

Figure 4. Current–voltage (*I–V*) relationship for a CO_2-sensitive current in isolated cultured gill neuroepithelial cells (NECs) of zebrafish (*Danio rerio*)
A, mean current–voltage (*I–V*) relationships during exposure to normoxia (Nox) or hypercapnia (Hpc) from 12 cells. Currents were evoked by changing the voltage from −90 mV to +60 mV following a ramp protocol from a holding potential of −60 mV (inset). Inset also shows representative current traces from a single NEC. *B*, mean *I–V* relationship of the CO_2-sensitive difference current (open symbols, Nox-Hpc) from 12 cells. The CO_2-sensitive difference current (I_{KCO_2}) reverses near E_K (calculated using bath and pipette K^+ concentrations) and fits the corresponding Goldman–Hodgkin–Katz current equation (GHK, continuous curve; Hille, 2001), suggesting that it is predominantly carried by K^+ ions.

treated with both 5HT and CA primary antibodies after CA preabsorption, only 5HT-IR was observed (Fig. 6*B*).

To directly examine the role of CA in the response of NECs to CO_2, NECs were exposed to isohydric hypercapnia (constant pH 7.4). Figure 6*C* and *D* show that typical hypercapnia-induced responses persisted in the absence of extracellular acidosis but were inhibited by the presence of 50 μM acetazolamide (a CA inhibitor). Acetazolamide reduced the magnitude of responses to a transient CO_2 stimulus by an average of 12 mV ($n = 6$ CO_2 sensitive NECs). Acetazolamide also delayed the time to reach peak membrane depolarization by an average of 10.5 s when comparing cells before and after drug treatment.

Discussion

The results of the present study provide the first direct evidence of CO_2 transduction in fish and demonstrate that the underlying mechanism involves inhibition of background K^+ channels via a pathway involving carbonic anhydrase. The finding that a sub-population of gill NECs act as sensors for both O_2 and CO_2 provides further support for the evolutionary link between the fish gill and

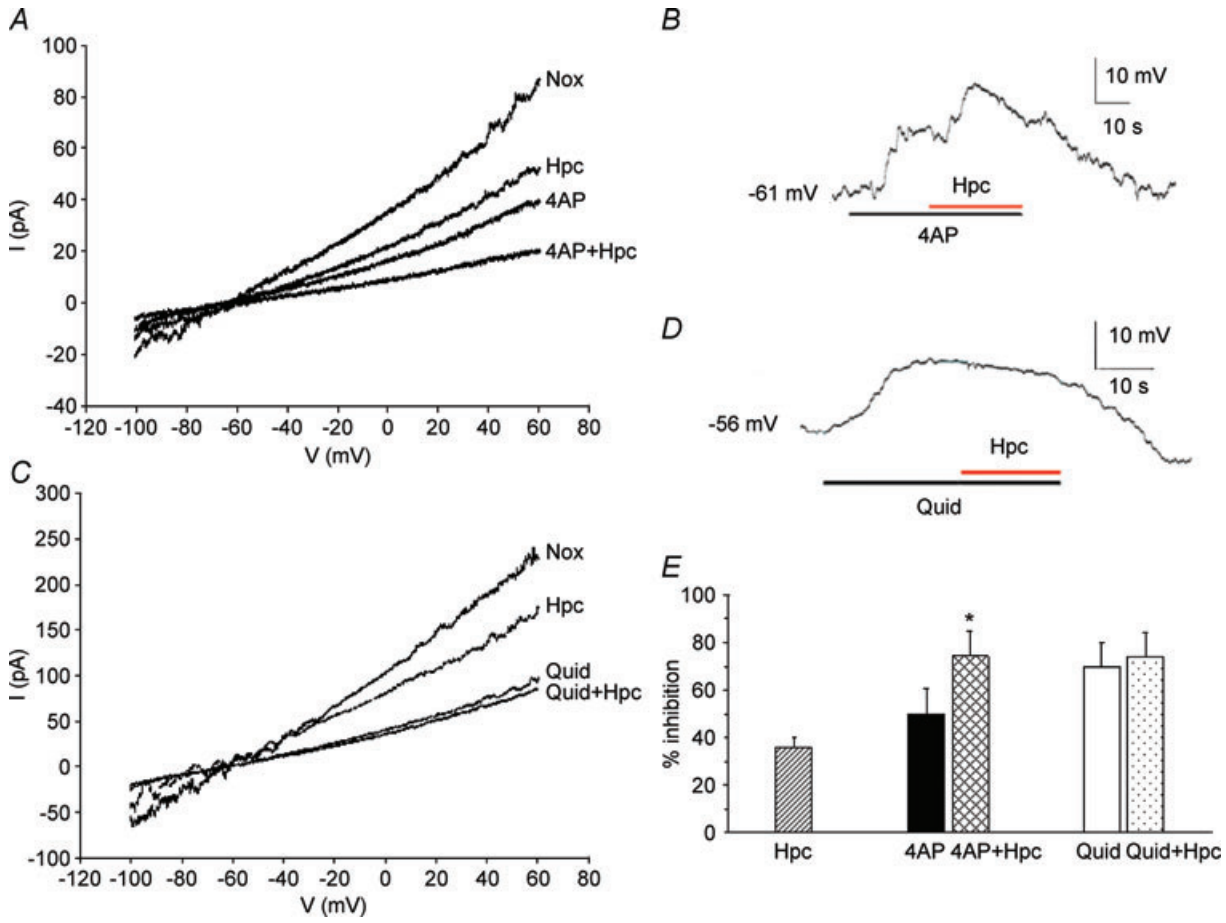

Figure 5. Pharmacological characteristics of CO_2 sensing in isolated cultured gill neuroepithelial cells (NECs) of zebrafish (*Danio rerio*)

A, average current–voltage (*I–V*) relationship of whole-cell voltage clamp recordings from five CO_2-sensitive NECs during exposure to normoxia (Nox), hypercapnia (Hpc), 4-AP and 4-AP+Hpc showing the persistence of the hypercapnic effects in the presence of 4-AP. Currents were evoked by changing the voltage from −100 mV to +60 mV following a ramp protocol (1 s) from a holding potential of −60 mV. *B*, typical current clamp recording of a reversible hypercapnic depolarization following application of 2.5 mM 4-AP. *C*, average current–voltage (*I–V*) relationship of whole-cell voltage clamp recordings from six CO_2-sensitive NECs during exposure to Nox, Hpc, quinidine (Quid) and Quid+Hpc; a ramp protocol was used (as in *A*). Hypercapnia (Hpc) reduced currents over a range of potentials, but had little effect in the presence of 0.5 mM quinidine (Quid+Hpc). *D*, typical current clamp recording showing the reversible depolarization following bath application of 0.5 mM quinidine, but subsequent hypercapnia having no additional affect. *E*, mean ± S.E.M. inhibition of whole-cell current at 50 mV using the data points in Fig. 4 as well as in panels A and C, showing hypercapnia effects alone (Hpc), hypercapnia effects in the presence of 4-AP (4AP, 4AP + Hpc, paired *t* test, $^*P < 0.05$) and quinidine (Quid, Quid+Hpc) respectively.

the carotid body in mammals. However, a major difference between the two CO_2-sensing structures is that the gill NECs are able to respond to absolute partial pressures of CO_2 approximately 10 times lower than the carotid body. The evolutionary significance of these different sensing thresholds is that each CO_2-sensing structure is exquisitely adapted to detect deviations in arterial blood P_{CO_2} from normal set points which in mammals and water-breathing fish are approximately 40 mmHg and 2–3 mmHg, respectively.

Electrophysiological properties of CO_2 sensitivity

Whole cell voltage and current clamp recordings, performed on isolated NECs, allowed us to investigate the electrophysiological responses to hypercapnia. Hypercapnia inhibited a CO_2 sensitive channel, resulting in a decrease in whole-cell conductance. The current mediated by this channel reversed near the equilibrium potential for K^+, displayed open rectification, and is well-described by the Goldman–Hodgkin–Katz current equation (Fig. 4). These findings are consistent with the effect of hypercapnia on membrane potential in rat carotid body glomus cells (Buckler & Vaughan-Jones, 1994*a*,*b*; Urena *et al.* 1994; Montoro *et al.* 1996). The involvement of a K^+ current in mediating CO_2 sensing is further supported by pharmacological data using K^+ channel blockers (Fig. 5).

Whole cell recording of NECs under voltage clamp revealed that the CO_2-dependent inhibition of outward current was not significantly affected by 4-AP; in the presence of 4-AP, hypercapnia resulted in a further 24% reduction in current. In contrast, CO_2-dependent inhibition was almost completely blocked by quinidine; additional hypercapnia was unable to cause further reduction in current in the presence of quinidine. These observations were corroborated under current clamp as well (Fig. 5*B* and *D*). Interestingly, these data are similar to the hypoxia-induced responses observed in other chemoreceptor cells, such as human neuroepithelial body-derived H-146 cells (O'kelly *et al.* 1999), carotid body glomus cells (Buckler, 1997; Buckler *et al.* 2000) and other peripheral neurons such as rat glossopharyngeal neurons (Campanucci *et al.* 2003). Generally speaking, the CO_2 sensitive current we describe possesses all the characteristics of a current mediated by background (or leak) K^+ channels, which show no voltage or time dependence (Bayliss *et al.* 2003; Buckler, 2007). However, further experiments will be required to determine the specific type of background K^+ channel involved in CO_2 sensing in gill NECs. In mammalian neuroepithelial sensory receptors (e.g. carotid body glomus cells), a background K^+ current causing membrane depolarization has been identified as a member of the TWIK (tandem P domain weakly inward-rectifying K^+)-related acid-sensitive K^+ (TASK) family (Buckler *et al.* 2000; Bayliss *et al.* 2003; Buckler, 2007). Moreover, TASK/TASK-like K^+ channels have been reported in other neurons (Nattie, 1999; Putnam *et al.* 2004; Buckler, 2007) including (1) central chemosensory neurons mediating CO_2 sensing in the brain, e.g. medullary raphe neurons (Wang *et al.* 2002; Washburn *et al.* 2002, 2003), ventral medulla neurons (Neubauer *et al.* 1991; Wellner-Kienitz & Shams, 1998) and locus coeruleus neurons (Bayliss *et al.* 2001); (2) respiratory motor neurons conveying central respiratory drive to the muscles of breathing (Nattie,

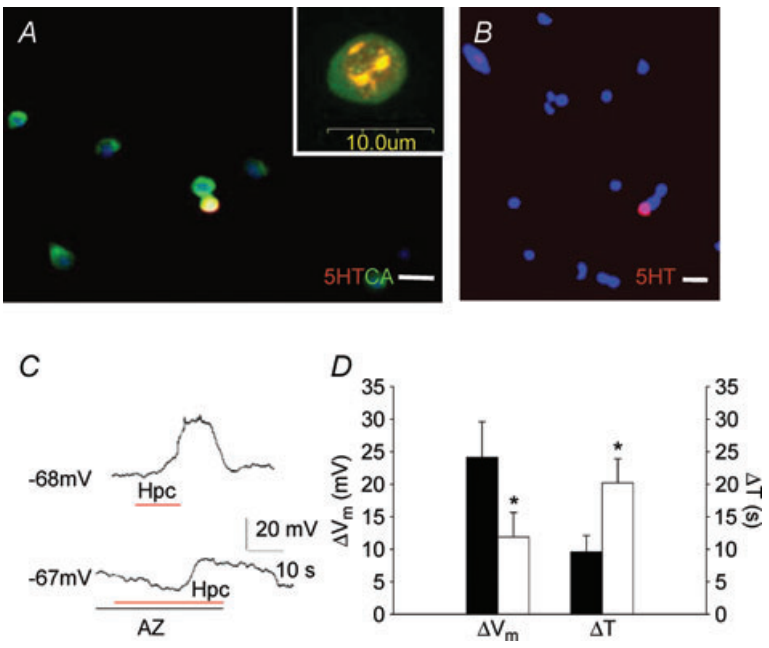

Figure 6. Effects of acetazolamide (AZ) on the CO_2-sensitive membrane potential in isolated cultured gill neuroepithelial cells (NECs) of zebrafish (*Danio rerio*)
A, representative image of 5HT-immunoreactive (IR; red) and/or CA-IR (green) NECs in primary cell culture. The cell nuclei appear as blue; yellow/orange represents co-localization of 5HT and CA. Note that all 5HT-IR cells exhibit CA-IR. In addition, some cells appeared to exclusively express CA, whereas other cells appeared to lack both 5HT and CA. Inset: confocal image of a cell colocalizing 5HT and CA. *B*, preabsorption of the CA antibody with excess CA followed by application of 5HT and CA antibodies yielded only 5HT-IR NECs. Scale bars = 20 μm in *A* (applies to *B* also). *C*, typical current-clamp recording of a reversible depolarization during perfusion with hypercapnic solution (upper trace) as well as a reduced and delayed depolarization after the administration of 50 μM acetazolamide (AZ) on the same cell (lower trace). *D*, mean ± S.E.M. ($n = 6$) membrane potential changes (ΔV_m) and time to peak depolarization (ΔT) during hypercapnia alone (ctrl; filled bars) and in the presence of 50 μM acetazolamide (AZ; open bars; paired *t* test, $^*P < 0.05$).

1999); and (3) other peripheral sensory neurons such as rat nociceptive cells (Cooper *et al.* 2004).

Carbonic anhydrase and CO_2 chemoreception in NECs

This study also investigated the involvement of carbonic anhydrase (CA) on CO_2 transduction. It was demonstrated that bath application of acetazolamide reversibly reduced the responses to a transient CO_2 stimulus, similar to observations in the carotid body glomus cells (Buckler *et al.* 1991*a*,*b*; Iturriaga *et al.* 1991; Iturriaga & Lahiri, 1993; Iturriaga, 1993), cat laryngeal cells (Coates *et al.* 1996), cat ventral medulla neurons (Coates *et al.* 1991) and isolated rat neonatal chromaffin cells (Munoz-Cabello *et al.* 2005). It would appear that CA activity in the zebrafish gill NECs, as in the carotid body, is important in setting the magnitude and speed of the initial response to an elevation of P_{CO_2}, presumably by accelerating the hydration reaction and thus the rate of intracellular acidification. The residual response of NECs to hypercapnia after CA inhibition presumably reflects intracellular acidification occurring at the uncatalysed rate of CO_2 hydration. Thus, although intracellular acidification would still occur in the absence of CA, its presence in CO_2-sensing cells allows a more rapid and vigorous response than otherwise might be possible.

Because the zebrafish NECs also respond to metabolic acidosis (reduced pH at constant P_{CO_2}; Z. Qin, J. Lewis & S. F. Perry, unpublished data), it was necessary to assess the role of CA using isohydric hypercapnia. This protocol served to exclude the CA-independent contribution of intracellular H^+ *not* arising from the inward diffusion of CO_2. It will be important to extend these results by directly measuring intracellular pH while exposing NECs to changes in P_{CO_2} in the presence or absence of acetazolamide. Additionally, future experiments should attempt to assess the relative involvement of extracellular *versus* intracellular acidosis in promoting membrane depolarization when NECs are exposed to hypercapnia.

Interaction between hypoxia and hypercapnia on NEC chemosensitivity

An important finding of the present study is that individual NECs can respond to both hypoxia and hypercapnia. Such bimodal sensing, also seen in the carotid body, suggests that reflex cardiorespiratory responses to hypercapnia and hypoxia are mediated, at least in part, by the same chemosensory cells. Thus, the transduction pathways for both O_2 and CO_2 coexist within a common primary receptor cell and might converge at or after the membrane depolarization. In carotid body glomus cells, both stimuli have been shown to elicit K^+ current inhibition, electrical activity, voltage-gated Ca^{2+} influx (Peers, 1990*a*,*b*; Peers & Green, 1991; Buckler & Vaughan-Jones, 1993, 1994*a*,*b*; Buckler, 1997; Dasso *et al.* 2000) and subsequent neurotransmitter release and afferent nerve activation (Lahiri & DeLaney, 1975; Zhang & Nurse, 2004). Therefore, the sensing of hypoxia and hypercapnia/acidosis involves common steps. There is also some evidence that the primary CO_2/pH sensor is independent of the O_2 sensor in some cases; the effects of CO_2 and/or pH are not mediated through changes in the affinity of an O_2 sensor in carotid body glomus cells (Dasso *et al.* 2000). However, there are also data suggesting that CO_2 chemosensitivity may be modulated by hypoxia (Reid *et al.* 2005; see review by Lahiri & Forster, 2003). It is interesting that while the glomus cells of the carotid body proliferate in response to chronic hypoxia, the density of the analogous population of gill NECs (those possessing 5-HT) in zebrafish is unaffected by long-term hypoxia (Jonz *et al.* 2004; Vulesevic *et al.* 2006). On the other hand, NECs not containing 5-HT (without a proven function) do display a significant proliferation upon exposure of zebrafish to chronic hypoxia (Jonz *et al.* 2004). Thus, in keeping with the lack of a robust response to chronic hypoxia, it is not surprising that the numbers of gill filament NECs remain unaltered by chronic hypercapnia (Vulesevic *et al.* 2006).

Although evidence has shown the membrane voltage response of zebrafish NECs to hypoxia closely resembles the discharge frequency in sensory fibres of the isolated trout gill preparations (Burleson & Milsom, 1993; Jonz *et al.* 2004), a direct link between CO_2-sensitive currents in NECs and sensory neuron discharge remains to be determined. A recent study of rat adrenal medulla chromaffin cells (Munoz-Cabello *et al.* 2005) which act as neonatal CO_2 sensors before complete maturation of peripheral and central chemoreceptors has linked hypercapnia-induced membrane depolarization to Ca^{2+}-dependent catecholamine secretion. Similar studies using a combination of patch clamp and amperometric techniques will be important for future chemotransduction studies in fish NECs.

Summary and perspectives

Exposure of fish to hypercapnia initiates several cardiorespiratory reflexes including hyperventilation, bradycardia, increased peripheral vascular resistance and catecholamine secretion (Perry *et al.* 1999; Perry & Reid, 2002; see reviews by Perry & Gilmour, 2002; Gilmour & Perry, 2007). In this study, we provide evidence that these reflexes may originate from the activation of branchial NECs that can function as bimodal CO_2 and O_2 chemoreceptors. The results demonstrate several similarities with mammalian peripheral chemoreceptors (i.e. carotid

body). This comparison suggests a phylogenetic trend whereby CO_2 chemoreception may first have arisen in the periphery to sense the external environment, and subsequently central chemoreception arose to monitor internal blood and optimize metabolism (Milsom, 2002).

While it is clear that zebrafish NECs respond to elevated CO_2 with membrane depolarization, further research is required to elucidate the specific signal transduction cascade and its downstream effects. Because the genetically tractable zebrafish displays CO_2 chemosensitivity at 3 days post-fertilization (L. Labonté and S. F. Perry, unpublished data), it should be feasible to assess cardiorespiratory responses *in vivo* and electrophysiological responses *in vitro* in fish (or in cells derived from fish) subjected to selective gene knockdown.

References

Bailly Y, Dunelerb S & Laurent P (1992). The neuroepithelial cells of the fish gill filament: indolamine-immunocytochemistry and innervation. *Anat Rec* **233**, 143–161.

Bayliss DA, Sirois JE & Talley EM (2003). The TASK family: two-pore domain background K^+ channels. *Mol Interv* **3**, 205–219.

Bayliss DA, Talley EM, Sirois JE & Lei Q (2001). TASK-1 is a highly modulated pH-sensitive 'leak' K^+ channel expressed in brainstem respiratory neurons. *Respir Physiol* **129**, 159–174.

Buckler KJ (1997). A novel oxygen-sensitive potassium current in rat carotid body type I cells. *J Physiol* **498**, 649–662.

Buckler KJ (2007). TASK-like potassium channels and oxygen sensing in the carotid body. *Respir Physiol Neurobiol* **157**, 55–64.

Buckler KJ, Williams BA & Honore E (2000). An oxygen-, acid- and anaesthetic-sensitive TASK-like background potassium channel in rat arterial chemoreceptor cells. *J Physiol* **525**, 135–142.

Buckler KJ & Vaughan-Jones RD (1993). Effects of acidic stimuli on intracellular calcium in isolated type I cells of the neonatal rat carotid body. *Pflugers Arch* **425**, 22–27.

Buckler KJ & Vaughan-Jones RD (1994*a*). Effects of hypercapnia on membrane potential and intracellular calcium in rat carotid body type I cells. *J Physiol* **478**, 157–171.

Buckler KJ & Vaughan-Jones RD (1994*b*). Effects of hypoxia on membrane potential and intracellular calcium in rat neonatal carotid body type I cells. *J Physiol* **476**, 423–428.

Buckler KJ, Vaughan-Jones RD, Peers C, Lagadic-Gossmann D & Nye PC (1991*a*). Effects of extracellular pH, PCO_2 and HCO_3^- on intracellular pH in isolated type-I cells of the neonatal rat carotid body. *J Physiol* **444**, 703–721.

Buckler KJ, Vaughan-Jones RD, Peers C & Nye PC (1991*b*). Intracellular pH and its regulation in isolated type I carotid body cells of the neonatal rat. *J Physiol* **436**, 107–129.

Burleson ML, Mercer SE & Wilk-Blaszczak MA (2006). Isolation and characterization of putative O_2 chemoreceptor cells from the gills of channel catfish (*Ictalurus punctatus*). *Brain Res* **1092**, 100–107.

Burleson ML & Milsom WK (1993). Sensory receptors in the first gill arch of rainbow trout. *Respir Physiol* **93**, 97–110.

Burleson ML & Smatresk NJ (2000). Branchial chemoreceptors mediate ventilatory responses to hypercapnic acidosis in channel catfish. *Comp Biochem Physiol A* **125**, 403–414.

Campanucci VA, Fearon IM & Nurse CA (2003). A novel O_2-sensing mechanism in rat glossopharyngeal neurones mediated by a halothane-inhibitable background K^+ conductance. *J Physiol* **548**, 731–743.

Coates EL, Li AH & Nattie EE (1991). Acetazolamide on the ventral medulla of the cat increases phrenic output and delays the ventilatory response to CO_2. *J Physiol* **441**, 433–451.

Coates EL, Knuth SL & Bartlett DJ (1996). Laryngeal CO_2 receptors: influence of systemic PCO_2 and carbonic anhydrase inhibition. *Respir Physiol* **104**, 53–61.

Cooper BY, Johnson RD & Rau KK (2004). Characterization and function of TWIK-related acid sensing K^+ channels in a rat nociceptive cell. *Neuroscience* **129**, 209–224.

Dasso LL, Buckler KJ & Vaughan-Jones RD (2000). Interactions between hypoxia and hypercapnic acidosis on calcium signalling in carotid body type I cells. *Am J Physiol Lung Cell Mol Physiol* **279**, L36–42.

Drummond GB (2009). Reporting ethical matters in *The Journal of Physiology*: standards and advice. *J Physiol* **587**, 713–719.

Dunel-Erb S, Bailly Y & Laurent P (1982). Neuroepithelial cells in fish gill primary lamellae. *J Appl Physiol* **53**, 1342–1353.

Esbaugh A, Perry SF, Bayaa M, Georgalis T, Nickerson JG, Tufts BL & Gilmour KM (2005). Cytoplasmic carbonic anhydrase isozymes in rainbow trout *Oncorhynchus mykiss:* Comparative physiology and molecular evolution. *J Exp Biol* **208**, 1951–1961.

Georgalis T, Perry SF & Gilmour KM (2006). The role of branchial carbonic anhydrase in acid-base regulation in rainbow trout (*Oncorhynchus mykiss*). *J Exp Biol* **209**, 518–530.

Gilmour KM (2001). The CO_2/pH ventilatory drive in fish. *Comp Biochem Physiol* **130**, 219–240.

Gilmour KM, Milsom WK, Rantin FT, Reid SG & Perry SF (2005). Cardiorespiratory responses to hypercarbia in tambaqui (*Colossoma macropomum*): chemoreceptor orientation and specificity. *J Exp Biol* **208**, 1095–1107.

Gilmour KM & Perry SF (2007). Branchial chemoreceptor regulation of cardiorespiratory function. In *Sensory Systems Neuroscience*, ed. Hara TJ & Zielinski B, pp. 97–151. Academic Press, San Diego.

Gilmour KM & Perry SF (2009). Carbonic anhydrase and acid-base regulation in fish. *J Exp Biol* **212**, 1647–1661.

Goniakowska-Witalinska L, Zaccone G, Fasulo S, Mauceri A, Licata A & Youson J (1995). Neuroendocrine cells in the gills of the bowfin *Amia calva*. An ultrastructural and immunocytochemical study. *Folia Histochem Cytobiol* **33**, 171–177.

Gonzalez C, Almaraz L, Obeso A & Rigual R (1994). Carotid body chemoreceptors: from natural stimuli to sensory discharges. *Physiol Rev* **74**, 829–898.

Gonzalez C, Almaraz L, Obeso A & Rigual R (1992). Oxygen and acid chemoreception in the carotid body chemoreceptors. *Trends Neurosci* **15**, 146–153.

Guyenet PG (2008). The 2008 Carl Ludwig Lecture: retrotrapezoid nucleus, CO_2 homeostasis, and breathing automaticity. *J Appl Physiol* **105**, 404–416.

Hamill OP, Marty A, Neher E, Sakmann B & Sigworth FJ (1981). Improved patch-clamp techniques for high-resolution current recording from cells and cell-free membrane patches. *Pflugers Arch* **391**, 85–100.

Hille B (2001). *Ion Channels of Excitable Membranes*, 3rd edn, Sinauer Associates, Sunderland, MA, USA.

Iturriaga R (1993). Carotid body chemoreception: the importance of CO_2-HCO_3^- and carbonic anhydrase. *Biol Res* **26**, 319–329.

Iturriaga R & Lahiri S (1993). Carbonic anhydrase and carotid body chemoreception in the presence and absence of CO_2-HCO_3^-. *Adv Exp Med Biol* **337**, 171–176.

Iturriaga R, Lahiri S & Mokashi A (1991). Carbonic anhydrase and chemoreception in the cat carotid body. *Am J Physiol Cell Physiol* **261**, C565–573.

Jonz MG, Fearon IM & Nurse CA (2004). Neuroepithelial oxygen chemoreceptors of the zebrafish gill. *J Physiol* **560**, 737–752.

Jonz MG & Nurse CA (2003). Neuroepithelial cells and associated innervation of the zebrafish gill: a confocal immunofluorescence study. *J Comp Neurol* **461**, 1–17.

Lahiri S & DeLaney RG (1975). Stimulus interaction in the responses of carotid body chemoreceptor single afferent fibres. *Respir Physiol* **24**, 249–266.

Lahiri S & Forster RE (2003). CO_2/H^+ sensing: peripheral and central chemoreception. *Int J Biochem Cell Biol* **35**, 1413–1435.

McKendry JE, Milsom WK & Perry SF (2001). Branchial CO_2 receptors and cardiorespiratory adjustments during hypercarbia in Pacific spiny dogfish (*Squalus acanthias*). *J Exp Biol* **204**, 1519–1527.

McKendry JE & Perry SF (2001). Cardiovascular effects of hypercapnia in rainbow trout (*Oncorhynchus mykiss*): A role for externally oriented chemoreceptors. *J Exp Biol* **204**, 115–125.

Milsom WK (2002). Phylogeny of CO_2/H^+ chemoreception in vertebrates. *Respir Physiol Neurobiol* **131**, 29–41.

Milsom WK & Burleson ML (2007). Peripheral arterial chemoreceptors and the evolution of the carotid body. *Respir Physiol Neurobiol* **157**, 4–11.

Milsom WK, Sundin L, Reid S, Kalinin A & Rantin FT (1999). Chemoreceptor control of cardiovascular reflexes. In *Biology of Tropical Fishes*, ed. Val AL & Almeida-Val VMF, pp. 363–374. INPA, Manaus, Brazil.

Montoro RJ, Urena J, Fernandez-Chacon R, Alvarez de Toledo G & Lopez-Barneo J (1996). Oxygen sensing by ion channels and chemotransduction in single glomus cells. *J Gen Physiol* **107**, 133–143.

Munoz-Cabello AM, Toledo-Aral JJ, Lopez-Barneo J & Echevarria M (2005). Rat adrenal chromaffin cells are neonatal CO_2 sensors. *J Neurosci* **25**, 6631–6640.

Nattie E (1999). CO_2, brainstem chemoreceptors and breathing. *Prog Neurobiol* **59**, 299–331.

Neubauer JA, Gonsalves SF, Chou W, Geller HM & Edelman NH (1991). Chemosensitivity of medullary neurons in explant tissue cultures. *Neuroscience* **45**, 701–708.

O'Kelly I, Stephens RH, Peers C & Kemp PJ (1999). Potential identification of the O_2-sensitive K^+ current in a human neuroepithelial body-derived cell line. *Am J Physiol Lung Cell Mol Physiol* **276**, L96–104

O'Regan RG & Majcherczyk S (1982). Role of peripheral chemoreceptors and central chemosensitivity in the regulation of respiration and circulation. *J Exp Biol* **100**, 23–40.

Peers C & Green FK (1991). Inhibition of Ca^{2+}-activated K^+ currents by intracellular acidosis in isolated type I cells of the neonatal rat carotid body. *J Physiol* **437**, 589–602.

Peers C (1990*a*). Effect of lowered extracellular pH on Ca^{2+}-dependent K^+ currents in type I cells from the neonatal rat carotid body. *J Physiol* **422**, 381–395.

Peers C (1990*b*). Hypoxic suppression of K^+ currents in type I carotid body cells: selective effect on the Ca^{2+}-activated K^+ current. *Neurosci Lett* **119**, 253–256.

Perry SF, Fritsche R, Hoagland T, Duff DW & Olson KR (1999). The control of blood pressure during external hypercapnia in the rainbow trout (*Oncorhynchus mykiss*). *J Exp Biol* **202**, 2177–2190.

Perry SF & Gilmour KM (2002). Sensing and transfer of respiratory gases at the fish gill. *J Exp Zool* **293**, 249–263.

Perry SF & McKendry JE (2001). The relative roles of external and internal CO_2 *versus* H^+ in eliciting the cardiorespiratory responses of *Salmo salar* and *Squalus acanthias* to hypercarbia. *J Exp Biol* **204**, 3963–3971.

Perry SF & Reid SG (2002). Cardiorespiratory adjustments during hypercarbia in rainbow trout (*Oncorhynchus mykiss*) are initiated by external CO_2 receptors on the first gill arch. *J Exp Biol* **205**, 3357–3365.

Putnam RW, Filosa JA & Ritucci NA (2004). Cellular mechanisms involved in CO_2 and acid signalling in chemosensitive neurons. *Am J Physiol Cell Physiol* **287**, C1493–526.

Reid SG, Perry SF, Gilmour KM, Milsom WK & Rantin FT (2005). Reciprocal modulation of oxygen and carbon dioxide cardiorespiratory chemoreflexes in the tambaqui (*Colossoma macropomum*). *Respir Physiol Neurobiol* **147**, 175–194.

Reid SG, Sundin L, Kalinin AL, Rantin FT & Milsom WK (2000). Cardiovascular and respiratory reflexes in the tropical fish, traira (*Hoplias malabaricus*): CO_2/pH chemoresponses. *Respir Physiol* **120**, 47–59.

Ryan JA (2005). Growing more cells: A simple guide to small volume cell culture scale-up. http://www.corning.com/Lifesciences/technical˙information/techDocs/cc_scale_up_guide.pdf. pp. 1–16. Corning Inc.

Saltys HA, Jonz MG & Nurse CA (2006). Comparative study of gill neuroepithelial cells and their innervation in teleosts and *Xenopus* tadpoles. *Cell Tissue Res* **323**, 1–10.

Smith FM & Jones DR (1978). Localization of receptors causing hypoxic bradycardia in trout (*Salmo gairdneri*). *Can J Zool* **56**, 1260–1265.

Sundin L, Reid SG, Rantin FT & Milsom WK (2000). Branchial receptors and cardiorespiratory reflexes in the neotropical fish, Tambaqui (*Colossoma macropomum*). *J Exp Biol* **203**, 1225–1239.

Urena J, Fernandez-Chacon R, Benot AR, Alvarez de Toledo GA & Lopez-Barneo J (1994). Hypoxia induces voltage-dependent Ca^{2+} entry and quantal dopamine secretion in carotid body glomus cells. *Proc Natl Acad Sci U S A* **91**, 10208–10211.

Vulesevic B, McNeill B & Perry SF (2006). Chemoreceptor plasticity and respiratory acclimation in the zebrafish, *Danio rerio*. *J Exp Biol* **209**, 1261–1273.

Wang W, Bradley SR & Richerson GB (2002). Quantification of the response of rat medullary raphe neurones to independent changes in pH_o and PCO_2. *J Physiol* **540**, 951–970.

Wellner-Kienitz MC & Shams H (1998). CO_2-sensitive neurons in organotypic cultures of the fetal rat medulla. *Respir Physiol* **111**, 137–151.

Washburn CP, Bayliss DA & Guyenet PG (2003). Cardiorespiratory neurons of the rat ventrolateral medulla contain TASK-1 and TASK-3 channel mRNA. *Respir Physiol Neurobiol* **138**, 19–35.

Washburn CP, Sirois JE, Talley EM, Guyenet PG & Bayliss DA (2002). Serotonergic raphe neurons express TASK channel transcripts and a TASK-like pH- and halothane-sensitive K^+ conductance. *J Neurosci* **22**, 1256–1265.

Zaccone G, Fasulo S, Ainis L & Licata A (1997). Paraneurons in the gills and airways of fishes. *Microsc Res Tech* **37**, 4–12.

Zaccone G, Lauweryns JM, Fasulo S, Tagliafierro G, Ainis L & Licata A (1992). Immunocytochemical localization of serotonin and neuropeptides in the neuroendocrine paraneurons of teleost and lungfish gills. *Acta Zool* **73**, 177–183.

Zaccone G, Mauceri A & Fasulo S (2006). Neuropeptides and nitric oxide synthase in the gill and the air-breathing organs of fishes. *J Exp Zoolog* **305**, 428–439.

Zaccone G, Tagliafierro G, Goniakowska-Witalinska L, Fasulo S, Ainis L & Mauceri A (1989). Serotonin-like immunoreactive cells in the pulmonary epithelium of ancient fish species. *Histochemistry* **92**, 61–63.

Zhang M & Nurse CA (2004). CO_2/pH chemosensory signalling in co-cultures of rat carotid body receptors and petrosal neurons: role of ATP and ACh. *J Neurophysiol* **92**, 3433–3445.

Author contributions

All authors had similar roles in the conception and design of experiments. Z.Q. performed the laboratory experiments and analysed the data. All authors contributed equally to the writing of the manuscript and to its final approval.

Acknowledgements

This study was financially supported by Natural Sciences and Engineering Research Council (NSERC) Discovery and Research Tools and Innovation grants to S.F.P. and J.L. J.L. was also supported by the Canadian Foundation for Innovation (CFI). We are grateful to Michael Jonz and Andrew Ochalski for invaluable assistance.